

LILAC: Layer-Wise Independent LoRAs and Cascaded Conditioning for Multi-Concept Customization of Diffusion Models

Marian Lupaşcu^{1,2}, Sebastian Ripă^{1,3}, Mihai Trăscău¹,
Mariana-Iuliana Georgescu¹, and Ionuţ Mironică¹

¹ Adobe Research, Romania

{lupascu, mtrascau, mgeorgescu, mironica}@adobe.com

² Department of Computer Science, University of Bucharest, Romania

³ International Computer High School of Bucharest, Romania

Abstract. Personalizing text-to-image diffusion models to render several specific subjects in a coherent image remains challenging: the model must preserve each subject’s identity while keeping the scene spatially and visually coherent. Methods that fuse independently trained concept adapters in a shared weight space (via federated averaging, gradient fusion, or orthogonality constraints) suffer from identity confusion and style bleeding and require joint retraining. In this work, we show that *composing concepts as separate image layers*, instead of merging their adapters in a shared weight space, *avoids parameter-level interference*. We introduce **LILAC**, a framework that composes independently trained low-rank adapters at inference time: each subject is conditioned on the frozen composite of previously placed subjects, with exactly one adapter active at a time, therefore identities never interfere at the parameter level. **LILAC** composes the adapters without any joint training, scales linearly with the number of concepts, and is backbone-agnostic. Under the Orthogonal Adaptation protocol, **LILAC** applied on Qwen-Image-Edit+Qwen-Image-Layered reaches an ArcFace detection rate of 0.861, while Orthogonal Adaptation reports 0.745 in its original setting. Code is available at <https://github.com/marianlupascu/LILAC>.

Keywords: Multi-concept personalization · Diffusion models · Low-rank adaptation · Layered generation · Identity preservation

1 Introduction

Parameter-efficient adaptation has made single-concept personalization of text-to-image diffusion models routine: a low-rank adapter (*e.g.* LoRA [6]) fine-tuned on a handful of images reliably captures one subject. Rendering several specific subjects in one coherent image is harder. The model must keep each identity while arranging the subjects plausibly and keeping the scene consistent. The standard recipe trains one adapter per concept and then combines these adapters in a shared parameter space, and this is where the difficulty concentrates. Once two concepts occupy the same weights their representations interfere: person-specific features blend, stylistic attributes leak across subjects, and one concept often dominates or suppresses another.

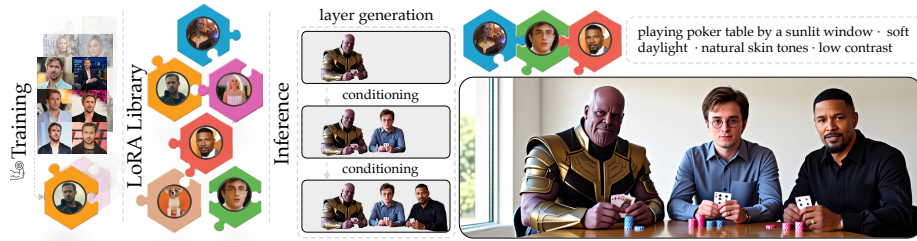


Fig. 1: Overview of **LILAC**. **Training** (left): Each concept is trained in isolation into a single LoRA adapter, building a library of independently trained, per-concept adapters. **LoRA Library** (center): Concepts trained independently, one per subject. **Inference** (right): **LILAC** selects a subset and renders every subject in one coherent scene from a text prompt. Exactly one adapter is active per pass under frozen conditioning, so identities never interfere at the parameter level, with no joint training and no weight merging. Each identity is preserved; in this example three subjects share a poker table by a sunlit window.

Existing remedies for combining adapters each trade one cost for another. Gradient fusion, as in Mix-of-Show [5], recovers fidelity at the price of per-composition optimization. Orthogonality constraints, as in Orthogonal Adaptation [12], enforce separation by retraining every concept under a shared scheme, and hold only up to the available rank budget as the number of concepts grows. None of these can reuse the many adapters already trained independently.

To mitigate weight-space interference while also using the existing adapters, we introduce **LILAC**, a framework that recasts multi-subject generation as a *layered synthesis* problem rather than a weight-merging one. Each concept is captured by an independently trained adapter, and subjects are composed one at a time at inference: the subjects are placed sequentially, every pass is conditioned on the frozen composite of the subjects already placed, and exactly one concept’s adapter is active. This per-concept binding has a decisive consequence. Because no two adapters are ever active together, the cross-concept crosstalk that orthogonality-based methods strive to minimize is never instantiated, and identities cannot interfere at the parameter level by construction. Geometric and photometric coherence between subjects instead emerges from the conditioning itself, with no auxiliary objective, no optimization loop, and no spatial supervision. **LILAC** requires no joint training and no optimization when concepts are composed, scales linearly in the number of subjects, and composes adapters trained in isolation, as shown in Fig. 1.

LILAC is backbone agnostic, therefore, we implement it on top of LaDe (a layered RGBA diffusion model) [10] and Qwen-Image-Edit+Qwen-Image-Layered [19]. For non-layered generative methods (Qwen-Image-Edit [18]), we propose the *scaffold* and *decomposition* techniques to enable the application of **LILAC**. We evaluate **LILAC** on the benchmark introduced by Orthogonal Adaptation [12], achieving an ArcFace detection rate of 0.861.

Our main contributions are: (i) we recast multi-concept customization as a layered, inference-time composition problem and introduce **LILAC**, a cascaded protocol that composes independently trained adapters without ever merging their

weights; (ii) a per-concept LoRA binding that eliminates cross-concept interference at the parameter level by construction, rather than minimizing it through a training-time orthogonality constraint; (iii) an empirical evaluation under the Orthogonal Adaptation protocol in which our configuration reaches an ArcFace detection rate of 0.861, against the ≤ 0.745 reported by merge-based baselines, with comparable concept and text fidelity and no weight merging.

2 Related Work

Subject-driven personalization. DreamBooth [15] fine-tunes the full backbone around a rare identifier token. Textual Inversion [4] optimizes a new token embedding while leaving the model frozen, while LoRA [6] injects low-rank weight increments that capture a concept at a fraction of the parameter cost. Later work refines what is adapted: B-LoRA [3], for instance, separates content and style by training only selected attention blocks. These methods produce a single high-quality adapter per concept, and a large community ecosystem of such adapters now exists. They do not, however, address how to place several independently learned concepts in one image, which is the problem we study.

Multi-concept customization by weight-space fusion. The prevailing approach to multi-concept generation combines per-concept adapters in a shared parameter space. Custom Diffusion [8] jointly optimizes a small set of weights over all concepts at once, while Mix-of-Show [5] tunes an embedding-decomposed LoRA per concept and merges them through gradient fusion. ZipLoRA [16] learns merge coefficients that combine a subject and a style adapter, and K-LoRA [11] selects in a training-free manner, the Top- K most important entries of each adapter in every attention layer. Orthogonal Adaptation [12] constrains independently trained adapters to occupy orthogonal subspaces, such that their residuals can be summed with reduced interference. Despite their differences, all of these methods represent multiple concepts in one set of weights. Due to their formulation, the residuals interact and identities can blend, while several additionally require joint training, a shared constraint, or per-composition optimization. ZipLoRA and K-LoRA target the subject-and-style pairing rather than multiple distinct subjects. Unlike the aforementioned methods, our LILAC *never forms a combined weight, therefore identities cannot interfere at the weight-level.*

Spatial and layout control. A second line of work composes concepts by specifying where to place them. Mix-of-Show [5] introduces regionally controllable sampling that binds each concept to a spatial region, GLIGEN [9] grounds generation on bounding boxes and layout tokens, and grid-based LoRA [1] composes concepts through a structured grid layout. OMG [7] explicitly targets occlusion between subjects in multi-concept generation. These methods achieve strong control, but they depend on explicit spatial supervision (masks, boxes, or layouts) supplied alongside the prompt. LILAC does not introduce such supervision: placement, scale, and interaction follow from the generation order and the frozen context alone, which also carries consistent lighting, and concept separation is enforced *structurally rather than spatially.*

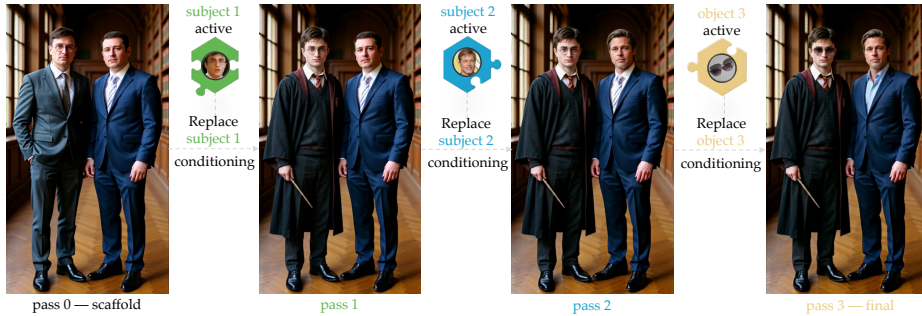


Fig. 2: Cascaded inference (scaffold configuration). Given an image (natural or generated), each concept is then added in its own pass with only its adapter active, conditioned on the frozen image of the concepts placed so far. No two adapters are active together, and earlier concepts and the background are preserved as later ones are added; the final pass adds a non-person concept (sunglasses), showing that the procedure composes objects and attributes as well as identities.

Layered and transparent generation. A body of work generates images as explicit layers. LayerDiffuse [20] encodes alpha transparency as a latent offset, turning a pretrained latent diffusion model into a generator of transparent RGBA layers and supporting foreground generation conditioned on a fixed background. Related approaches synthesize coordinated foreground and background layers or multiple transparent layers jointly, and recent models recover an arbitrary number of semantically disentangled RGBA layers from a single image [19]. LaDe [10] generates multiple semantically distinct RGBA layers within a single model, conditioning each layer on those already produced. We build directly on this capability (our backbone is a layered diffusion model of this kind), but the layered models themselves target the generation of transparent assets, not the identity-preserving composition of several independently trained concepts. Our contribution is the *cascaded, per-concept-bound protocol that turns single-layer conditional generation into scalable multi-subject customization*.

3 Method

Our key observation is that **multi-subject generation** does not require concepts to be combined in a shared weight space at all. We propose to treat it instead **as a layered synthesis problem**: each concept is captured by an adapter, and subjects are composed at inference time by rendering them on separate transparent layers and conditioning each generation on the layers produced. This novel recasting removes the source of cross-concept interference that affects weight-space fusion while requiring no joint training and no optimization at composition time. Fig. 2 details the cascaded inference procedure.

3.1 Overview

Given N concepts, each described by a small set of reference images X_k , our goal is to synthesize a single image that contains all N subjects with their individual identities preserved and their interactions natural, using only inference-time

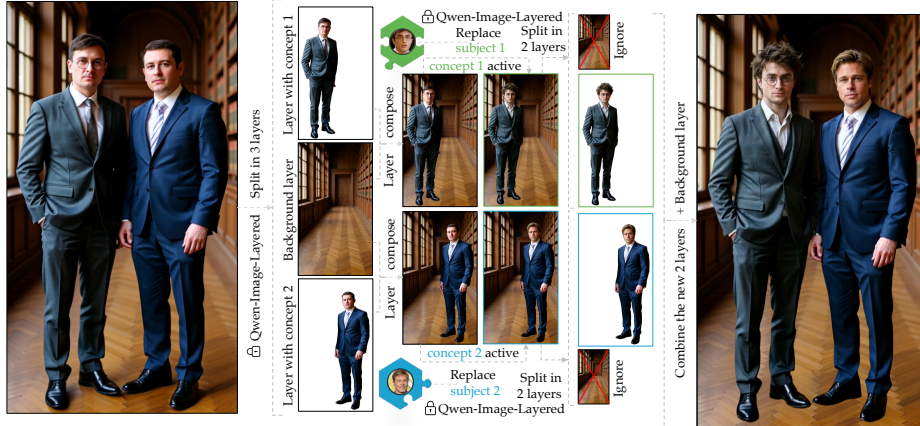


Fig. 3: Decomposition configuration on Qwen-Image-Edit [18]. Given an input image, Qwen-Image-Layered [19] then splits it into RGBA layers, here a background and two subject layers. Each subject is regenerated in its own pass: the frozen background is added as context, the placeholder subject is replaced with that concept’s adapter active, and the background is dropped to recover a transparent subject layer. The background carries no adapter and stays unchanged throughout, then recombines with the two regenerated subject layers into the final image. Because the per-subject layer come from a layer split rather than a direct edit, this route inherits any error in the split, so it preserves identity less reliably than the scaffold configuration (Sec. 4.2).

computation. Our method comprises three components: an independent adapter is trained for each concept (Sec. 3.2); the concepts are assigned to ordered layers (Sec. 3.3); and a cascaded inference procedure composes them on transparent layers (or images) under frozen conditioning (Sec. 3.4). We analyze the resulting isolation property in Sec. 3.5.

The method is defined over a layered diffusion backbone. Formally, we assume a backbone $\mathfrak{B} = \langle \theta, E, D \rangle$ that exposes three operations: an encoder E and decoder D for transparent RGBA layers; a conditional sampler $\text{Sample}(\cdot)$ that generates a layer from noise and a text prompt, optionally conditioned on a clean layer or composite; and weights θ that admit low-rank adaptation.

LILAC turns single-layer conditional capability (provided by the layered diffusion backbone) into identity-preserving multi-subject generation. Per-concept binding keeps each identity governed by its own adapter and the cascade composes an arbitrary number of subjects from independently trained adapters without merging them.

3.2 Independent Per-Concept LoRA Training

For each concept c_k we train a dedicated low-rank adapter on its reference set X_k while keeping the backbone frozen. The adapter modifies a pretrained weight $W_0 \in \mathbb{R}^{d \times d}$ through a low-rank increment,

$$W_0 + \Delta W_k, \quad \Delta W_k = B_k A_k, \quad (1)$$

with $B_k \in \mathbb{R}^{d \times r}$, $A_k \in \mathbb{R}^{r \times d}$, and $\text{rank } r \ll d$, so that the per-concept storage and the adaptation cost remain small. We optimize only the adapter parameters by minimizing the backbone’s native generative objective $\ell_{\mathfrak{B}}$ on the concept’s images X_k ,

$$\min_{B_k, A_k} \mathbb{E}_{x \sim X_k} [\ell_{\mathfrak{B}}(x; \theta, \Delta W_k, p_k)], \quad (2)$$

where θ are the parameters of the base model, ΔW_k are the adapter weights, and p_k is a caption that binds the concept c_k to a unique identifier token.

The defining feature of this stage is that it is performed independently for every concept. No concept is aware of any other during training: there is no joint optimization, no shared basis, and no orthogonality or separation constraint coupling the adapters. This decoupling is what later allows the cascade to combine arbitrary adapters at inference while keeping each identity governed solely by its own adapter (Sec. 3.5).

3.3 Layer Assignment and Anchor Selection

Before running the cascade explained in Sec. 3.4, the concepts must be assigned (or ordered): an assignment maps each concept to a layer index in $\{1, \dots, N\}$, with the concept at index 1 serving as the anchor. Therefore, c_1 is generated first and c_k is generated at step k . Unlike the adapters, the assignment is a design choice rather than a learned component, and it can be fixed before the inference. Because each subject is generated conditioned by the previous concepts, earlier concepts shape the placement, scale, and interaction of later ones, and the anchor, in particular, fixes the global composition for the entire scene. In the typical case the order follows directly from the prompt or from an explicit user specification. Therefore, we treat the choice of ordering as a hyperparameter whose effect we analyze in Supplementary sec. D, where the composition order proves to have only a minor effect.

3.4 Cascaded Inference with Frozen Layer Conditioning

The core of our method is an inference-time procedure that composes multiple subjects additively in layer space rather than in weight space, without requiring retraining or joint optimization. Given the per-concept adapters $\{\Delta W_k\}_{k=1}^N$ from Sec. 3.2, we generate the subjects one at a time: each concept is rendered on a RGBA layer (or image as in Fig. 2), and once produced that layer (image) is frozen and reused as a fixed conditioning context for every subsequent pass. We leverage this frozen context to enforce geometric and photometric consistency across subjects, while keeping each identity governed by a single adapter. Throughout, we write $\epsilon_{(k)} := \epsilon_{\theta_0 + \Delta W_k}$ for the backbone with only the k -th increment applied, and analyse the weight-level isolation it provides in Sec. 3.5. We begin with the concept assigned to layer $k = 1$ in Sec. 3.3, which we call the anchor. It is generated first and without conditioning, so that it establishes the global composition, the dominant pose, scale, and illumination to which the remaining subjects conform:

$$\hat{z}_1 = \text{Sample}(\epsilon_{(1)}; x_T, p_1, \emptyset), \quad L_1 = D(\hat{z}_1), \quad (3)$$

Algorithm 1: Cascaded inference with frozen layer conditioning

Input: adapters $\{\Delta W_k\}_{k=1}^N$ in generation order; prompts $\{p_k\}$; frozen backbone $\mathfrak{B} = \langle \epsilon_\theta, E, D \rangle$

Output: multi-subject image I ; per-subject layers $\{L_k\}_{k=1}^N$

```

1  $\mathcal{C}_0 \leftarrow \emptyset$  // empty (transparent) canvas
2 for  $k \leftarrow 1$  to  $N$  do
3    $x_T \sim \mathcal{N}(0, \mathbf{I})$  // fresh noise
4    $z^c \leftarrow E(\mathcal{C}_{k-1})$  // clean scaffold latent ( $\emptyset$  if  $k=1$ )
5    $\epsilon_{(k)} \leftarrow \epsilon_{\theta_0 + \Delta W_k}$  // bind only concept  $c_k$ 
6    $\hat{z}_k \leftarrow \text{Sample}(\epsilon_{(k)}; x_T, p_k, z^c)$ 
7    $L_k \leftarrow D(\hat{z}_k)$  // new RGBA layer
8    $\mathcal{C}_k \leftarrow L_k \oplus \mathcal{C}_{k-1}$  // freeze & accumulate
9 end
10  $I \leftarrow \mathcal{C}_N$ 
11 return  $I, \{L_k\}_{k=1}^N$ 

```

where $x_T \sim \mathcal{N}(0, \mathbf{I})$ is the initial latent and p_1 the anchor prompt. The resulting layer L_1 carries an alpha matte α_1 that delimits the anchor’s spatial support and leaves the remainder of the canvas transparent.

Once a layer is produced it is frozen: its pixels and alpha matte are fixed and never revisited. To condition the next generation on it, we alpha-composite all frozen layers into a single image and encode that image into a clean, noise-free latent,

$$\mathcal{C}_{k-1} = L_{k-1} \oplus \mathcal{C}_{k-2}, \quad \mathcal{C}_0 = \emptyset, \quad z_{k-1}^c = E(\mathcal{C}_{k-1}), \quad (4)$$

where \oplus denotes the alpha-over operator and \mathcal{C}_0 is an empty canvas. Because z_{k-1}^c is encoded directly from an image and supplied at the clean ($t = 0$) end of the process rather than as a noisy intermediate, the sampler treats it as a fixed exogenous context to be conditioned on, not as a signal to be denoised.

Concretely, the clean latent z_{k-1}^c is supplied to the sampler through the backbone’s reference-conditioning channel. Since we employ two different architecture layered diffusion models, their precise conditioning is described in Sec. 4.1.

Each remaining concept c_k , with $k \in \{2, \dots, N\}$, is then synthesised in a new step (as illustrated in Fig. 2) that activates only ΔW_k and takes the previously generated image as its conditioning signal:

$$\hat{z}_k = \text{Sample}(\epsilon_{(k)}; x_T, p_k, z_{k-1}^c), \quad L_k = D(\hat{z}_k), \quad \mathcal{C}_k = L_k \oplus \mathcal{C}_{k-1}, \quad (5)$$

with x_T redrawn at every pass.

The conditioning latent z_{k-1}^c encodes the position, scale, pose, and lighting of all subjects placed so far, therefore geometric and photometric coherence emerge from the conditioning itself, with no auxiliary objective.

After all N layers are generated, the final image is their alpha composite,

$$I = \mathcal{C}_N = L_N \oplus L_{N-1} \oplus \dots \oplus L_1. \quad (6)$$

The procedure integrates seamlessly with any layered backbone \mathfrak{B} that exposes the operations of Sec. 3.1. **LILAC** leaves the backbone frozen, retrains no adapter,

and takes no gradient step at composition. While we describe the cascade in its layered form, it relies only on these abstract operations. For example, on a backbone without native transparency, the frozen prior is supplied through an image-editing channel rather than as an intact RGBA layer, and the per-concept binding is unchanged in either case (Sec. 4.1). Its only added cost is N sequential sampling passes, linear in the number of subjects.

Algorithm 1 summarizes the complete routine.

The equations above describe the cascade in its native layered form, where each subject is generated directly on its own RGBA layer, with a single adapter active per layer, and conditioned on the frozen composite of the layers already produced. A backbone trained for layered generation performs this protocol directly. A standard image generation model cannot generate a subject as a conditional transparent layer, so we implement the same cascade in one of two ways.

In the *scaffold* configuration, the first pass generates a complete scene populated with generic placeholder figures in the intended arrangement (or a natural image can be used instead), fixing every subject’s placement at once, and each concept pass then *replaces* one placeholder with its subject through an image-editing pass that takes the frozen scene as its conditioning context and activates only that concept’s adapter. This approach is illustrated in Fig. 2.

In the *decomposition* configuration, given a generated or natural image, an off-the-shelf decomposer (Qwen-Image-Layered [19]) splits it into RGBA layers, and each person layer is then re-rendered with its concept adapter and alpha-composited back. The *decomposition* operation is illustrated in Fig. 3.

Both share the per-concept binding and frozen conditioning of Eq. (5) and differ only in how the layers are obtained. Because the scaffold commits to all placements before any identity is inserted and edits the rendered scene directly, it preserves identities more reliably, whereas the decomposition route inherits any error made by the layer split. We therefore adopt the scaffold configuration as our default and report the decomposition realization for comparison (Sec. 4.2).

3.5 Per-Layer LoRA Binding: Zero Interference by Construction

A defining property of our procedure is that the identity of each subject is governed by a single adapter that never shares the active parameter space with another. During the pass that generates concept c_k , the backbone operates with exactly one increment applied, $\epsilon_{(k)} = \epsilon_{\theta_0 + \Delta W_k}$, so that the adapted weights are $W_0 + \Delta W_k$ and no other concept contributes to the computation. We refer to this as per-layer LoRA binding, and show below that it removes cross-concept interference at the parameter level by construction, rather than reducing it through a training-time constraint.

Weight-space fusion methods take the opposite route. To place several concepts in one model they form a single merged weight,

$$\underbrace{W_0 + \sum_{k=1}^N \Delta W_k}_{\text{weight-space fusion}} \quad \text{vs.} \quad \underbrace{W_0 + \Delta W_k}_{\text{ours, pass } k}, \quad (7)$$

in which the residuals of distinct concepts act jointly on the same activations. Prior work quantifies the resulting interference through the crosstalk $\chi_{ij} = \|\Delta W_i^\top \Delta W_j\|_F$ between residuals $i \neq j$, and preserves identity by driving χ_{ij} toward zero. Orthogonal Adaptation [12], for instance, constrains the adapters to a shared orthogonal basis so that $\Delta W_i^\top \Delta W_j \approx 0$. Such constraints can only approximate the ideal, and their effectiveness is bounded by the available rank budget as the number of merged concepts grows. Independently trained adapters are, in fact, not orthogonal: across the person concepts of Sec. 4.1, the mean pairwise overlap between residual subspaces is 0.106 (Fig. 7; normalised to $[0, 1]$, with 0 denoting orthogonality), $5.3\times$ the 0.020 chance level measured for random adapters of the same per-layer dimensionality, so χ_{ij} is non-negligible and orthogonality must be actively imposed rather than assumed.

Per-layer binding sidesteps this trade-off entirely. Because the merged sum on the left of Eq. (7) is never formed, for every pair $i \neq j$ the two adapters are never simultaneously active, so the crosstalk χ_{ij} is not minimized but eliminated: it is never instantiated. The failure modes of fused models, identity confusion, style bleeding, and semantic entanglement, are thus removed structurally, independently of how the adapters were trained. On a layered backbone the separation is reinforced at the output level by the RGBA layering of Sec. 3.4, where each subject occupies a dedicated alpha-bounded layer; on a non-layered backbone it holds at the parameter level, the property established above.

This guarantee concerns parameter-level interference, not the absence of interaction between subjects. Subjects still influence one another, but only through the frozen conditioning of Sec. 3.4, which carries layout, scale, and lighting through the backbone’s cross-attention over a clean signal.

Two consequences follow. First, because no shared training scheme or orthogonality constraint is imposed, each adapter is an single-concept LoRA that can be trained, reused, and still composed at inference, unlike methods that require all concepts to be trained jointly. Second, the guarantee is invariant to the number of subjects (adding a concept adds a pass, never a cross term), so per-subject fidelity is not eroded as subjects accumulate, which we examine in Sec. 4.4.

4 Experiments

4.1 Experimental Setup

Backbones. Because our method only assumes a backbone that can condition a generation on a fixed prior and apply a concept adapter (Sec. 3.1), we validate it on two backbones of different kinds. The first is an open-source configuration built on Qwen-Image and Qwen-Image-Edit [18]. This backbone does not generate transparent layers conditionally, so we evaluate both image scaffold and decomposition configurations presented in Sec. 3.4. In the image-scaffold configuration, given a placeholder scene (generated or natural), each subject is then inserted by a Qwen-Image-Edit pass that takes the frozen scene as its source image, with that concept’s adapter as the only one active, as illustrated

in Fig. 2. In the decomposition configuration, the scene is split into RGBA layers by Qwen-Image-Layered [19], and each person layer is re-rendered with its adapter and recomposited, as illustrated in Fig. 3. Each adapter is trained with a blank source image (Sec. 3.2), which forces identity into the text-conditioned pathway, so at inference the source channel carries only the existing scene while the adapter contributes the new identity through its trigger token.

The second backbone is LaDe [10], a native layered backbone that generates every subject directly on a true RGBA layer, with a single adapter active per layer, and conditions on the intact frozen composed layers.

Validating the identical protocol on a plain image-editing model and on a native layered model isolates the contribution of the cascade and the binding from that of any single backbone, and shows that the protocol transfers even to a backbone with no native notion of layers.

Concepts and evaluation. We adopt the evaluation protocol and the concept bank of Orthogonal Adaptation [12]. Each concept is defined by a small set of reference images and trained into an independent adapter (Sec. 3.2); we form multi-subject groups by drawing concepts at random and render each group as a landscape (3:1) scene, following [12]. We report every metric over a fixed set of randomly formed groups and seeds per configuration. Before composition we screen each concept for single-concept fidelity and exclude any that fails, which separates multi-subject interference from single-concept training failures (Supplementary sec. B).

Metrics. We measure three complementary quantities, following the protocol of Orthogonal Adaptation [12]. *Identity preservation* (ID) is the ArcFace [2] detection rate: for each subject we take the highest cosine similarity between its detected face and its reference faces, count the subject as preserved when this exceeds the threshold of [12] (cosine > 0.32 , i.e. ArcFace distance < 0.68), and report the fraction of subjects preserved. This matches the identity-alignment metric of [12], which records an ArcFace detection below the same 0.68 distance and reports the detection probability rather than the raw distance. *Concept fidelity* (IA) is the CLIP-I [13] cosine similarity between each subject’s cropped region and its reference images, averaged over subjects. *Text alignment* (TA) is a CLIPScore of the composed image against the joint prompt: $\max(0, \cos) \times 2.5$ on the CLIP-T [13] cosine (CLIPScore [14]), the convention also used by [12]. Reporting identity and concept fidelity per subject, rather than only over the full image, detect the identity blending to which weight-space fusion is prone.

Baselines. Our quantitative comparison covers the multi-concept methods reported by Orthogonal Adaptation [12] on this exact concept bank and protocol: extended textual conditioning (P+ [17]), joint fine-tuning (Custom Diffusion [8]), DreamBooth-LoRA merged by federated averaging (DB-LoRA [6, 15]), gradient-based fusion (Mix-of-Show [5]), and orthogonality-constrained training (Orthogonal Adaptation [12]).



Fig. 4: Qualitative multi-subject comparison on the Orthogonal Adaptation bank [12]. Each pair of rows shows Orthogonal Adaptation [12] (top) and LILAC in its scaffold configuration (bottom) on the same prompt. The groups vary in size and combine a broad range of concepts, including real public figures, stylized fictional characters, animals, and accessories, placed in diverse scene contexts.

Implementation details. The full adapter, optimization, sampling, and model configuration is given in Supplementary sec. B.

4.2 Multi-Subject Comparison

Tab. 1 reports LILAC against the multi-concept baselines under the concept bank, metrics, and protocol of Supplementary sec. B; baseline numbers are quoted from the SDXL results of [12], so absolute values are comparable in scale but indicative across backbones (Sec. 5).

Two patterns stand out. First, on Identity, the merge-based baselines either collapse at composition (DB-LoRA drops to 0.098, $\Delta -0.585$) or, in the best case, hold roughly flat (Orthogonal Adaptation, 0.745, $\Delta +0.005$). LILAC instead reaches 0.861 in its scaffold configuration and 0.877 on the layered backbone, the two highest scores in the table. Second, the composition gap Δ separates the two failure modes from ours: a large negative Δ signals identity loss at merge time, while LILAC on the layered backbone stays essentially flat ($\Delta -0.002$), confirming that adding a subject adds a pass, not a cross term (Sec. 3.5). Text and image fidelity remain comparable to the strongest baseline across all configurations. We note that absolute identity is also lifted by the stronger single-concept backbone (LILAC starts from 0.961 single-concept versus 0.740 for the SDXL baselines), so the cross-backbone comparison should be read together with Δ rather than from the headline number alone.

Crucially, this holds on the same backbone. Run on Qwen-Image-Edit, the backbone LILAC uses, Orthogonal Adaptation collapses at three subjects to an

Table 1: Multi-subject comparison on the Orthogonal Adaptation concept bank and protocol [12], for each metric we give the single-concept score (*Single*), the multi-concept score (*Multi*), and their difference (Δ). For the weight-merging baselines, *Multi* is the post-merge result and Δ is the merge-induced change; **LILAC** performs no weight merging (merge time *none*), so its Δ is the single-concept-to-multi-subject composition gap rather than a merge cost. **LILAC** is reported on Qwen-Image-Edit [18] (decomposition, scaffold) and on a native layered backbone (LaDe [10]), so absolute values are indicative across backbones. Top-block baseline numbers are quoted directly from Table 2 of [12] (SDXL). We additionally re-run Orthogonal Adaptation on Qwen-Image-Edit, the same backbone as **LILAC**, for a controlled same-backbone comparison. Within each backbone, the best *Multi* per metric among **LILAC** configurations is in bold.

Method	Merge time	Text \uparrow			Image \uparrow			Identity \uparrow		
		Single	Multi	Δ	Single	Multi	Δ	Single	Multi	Δ
P+ [17]	<1 s	0.643	0.643	—	0.683	0.683	—	0.515	0.515	—
Custom Diffusion [8]	~2 s	0.668	0.673	+0.005	0.648	0.623	-0.025	0.504	0.408	-0.096
DB-LoRA (FedAvg) [6, 15]	<1 s	0.613	0.682	+0.069	0.744	0.531	-0.213	0.683	0.098	-0.585
Mix-of-Show (FedAvg) [5]	<1 s	0.625	0.621	-0.004	0.745	0.735	-0.010	0.728	0.706	-0.022
Mix-of-Show (Grad. Fusion) [5]	~15 m	0.625	0.631	+0.006	0.745	0.729	-0.016	0.728	0.717	-0.011
Orthogonal Adaptation (SDXL) [12]	<1 s	0.624	0.644	-0.010	0.748	0.741	-0.007	0.740	0.745	+0.005
Orthogonal Adaptation (Qwen) [12]	<1 s	0.750	0.664	-0.086	0.750	0.869	+0.119	0.929	0.000	-0.929
LILAC (decomposition)	none	0.754	0.734	-0.020	0.746	0.743	-0.003	0.961	0.639	-0.322
LILAC (scaffold)	none	0.754	0.711	-0.043	0.746	0.738	-0.008	0.961	0.861	-0.100
LILAC (LaDe)	none	0.759	0.758	-0.001	0.761	0.745	-0.016	0.879	0.877	-0.002

ArcFace detection rate of 0.000 (ID Δ -0.929), versus 0.861 for **LILAC** scaffold. The failure is specific to identity: image alignment even rises (IA 0.869). We attribute this to the orthogonal increments acting jointly over the full token sequence of the transformer, rather than over disjoint spatial regions, which yields plausible but blended faces: CLIP-based IA still scores them as the right kind of person, while ArcFace rejects each as a biometric match. This is the parameter-level interference **LILAC** removes by construction (Sec. 3.5), and it shows that on this backbone IA alone is misleading while identity exposes the merge failure.

4.3 Qualitative Results

Fig. 4 shows multi-subject compositions over diverse concept types: real public figures, fictional characters, animals, and accessories, in different scene styles. **LILAC** preserves each identity and keeps the subjects distinct. The subjects are placed coherently, with consistent lighting and plausible arrangement. The four-dog group and the subject wearing sunglasses show that the binding is not specific to faces, and composes objects and attributes as well. Fig. 5 shows further compositions across a range of subject counts, scene styles, and interactions.

Scaffold vs. decomposition. On Qwen-Image and Qwen-Image-Edit [18], the two implementations of Sec. 3.4 differ only in how the per-subject layers are obtained. The scaffold configuration (Fig. 2), which edits subjects into a rendered scene, preserves identity markedly more reliably than the decomposition configuration (Fig. 3, which first splits a generated scene into RGBA layers

with Qwen-Image-Layered [19]): in Tab. 1 scaffold reaches an ArcFace detection rate of 0.861 against 0.639 for decomposition, at a small cost in text and image alignment. The gap is consistent with errors introduced by the layer split, which the downstream identity edit cannot recover. We therefore treat scaffold as our default and report decomposition only for comparison.

4.4 Scalability

Because the per-concept binding of Sec. 3.5 adds a sampling pass (never a cross term) each time a subject is added, the per-subject quality of a composition should not collapse as the number of subjects N grows. Fig. 8 reports concept fidelity (CLIP-I), text alignment (CLIP-T), and identity (ArcFace detection rate) against N for the scaffold configuration, using random subject groups at each N . Concept fidelity and text alignment stay essentially flat from $N=1$ to $N=4$ (0.71–0.75 and 0.71–0.76): the appearance of each subject and the adherence to the prompt do not degrade as subjects are added. The ArcFace detection rate is lower and considerably noisier at larger N (per-group standard deviations above 0.2) and does not follow a clean monotone trend. We attribute this to scene crowding and to smaller, more frequently occluded faces at higher N , a face-detection effect, rather than to identity blending, which the per-concept binding removes by construction (Sec. 3.5): each subject is still rendered while a single adapter is active.

Inference cost. The cost of a composition is linear in the number of subjects: it runs N diffusion passes for the native layered cascade and $N+1$ for the scaffold configuration, each pass a single generation. On one H200, at 30 steps and 1536×512 , a pass takes 32.9s on average (almost independent of N), so a two-, three-, and four-subject scaffold composition takes 99, 132, and 165s respectively (3, 4, and 5 passes). This is the price LILAC pays for avoiding weight merging: the merging baselines amortize a one-time merge cost (Tab. 1, from under a second to roughly fifteen minutes for gradient fusion) and then generate in a single pass, whereas LILAC performs no merge but repeats the pass once per subject. When only a few images are needed per concept combination, or when the adapters have never been merged together before, trading merge time for inference time is favorable; reducing the per-subject pass count is a natural direction for future work.

5 Limitations

Composing subjects sequentially under frozen conditioning has clear boundaries. Because a frozen layer cannot be modified by a later pass, LILAC handles ordered occlusion naturally but struggles with close mutual occlusion and physical contact, where two subjects must interpenetrate or wrap around one another; these are its most challenging cases. On the Qwen-Image-Edit framework, where each pass re-encodes and edits the running composite rather than holding intact layers, repeated passes can also accumulate small changes to earlier subjects,



Fig. 5: Additional multi-subject compositions produced by LILAC. Each panel shows one generated scene; the circular thumbnails above it are the reference identities of the composed concepts, one per subject. The examples span two to three subjects and mix real public figures, stylized fictional characters, and animals, placed across varied scenes, styles, and interactions (side by side, shaking hands, toasting, conversing).

a drift that the native layered backbone avoids by keeping prior layers fixed. Finally, the method trades additional sampling time for its simplicity, since it runs N sequential passes; we view reducing this cost, and improving contact-rich interactions, as natural directions for future work.

6 Conclusion

We presented LILAC, a method for multi-subject personalized generation that composes independently trained concept adapters without merging their weights. By binding exactly one adapter per pass and conditioning each generation on the frozen composite of the subjects placed so far, LILAC removes cross-concept interference at the parameter level by construction, needs no joint training or per-composition optimization, scales linearly in the number of subjects, and composes adapters trained in isolation. We validated the same protocol on an open-source image-editing model and a native layered diffusion model under the evaluation protocol of Orthogonal Adaptation, showing that recasting multi-concept generation as layered, inference-time composition is a practical alternative to weight-space fusion.

References

1. Abdal, R., Patashnik, O., Deyneka, E., Chen, H., Siarohin, A., Tulyakov, S., Cohen-Or, D., Aberman, K.: Zero-shot dynamic concept personalization with grid-based lora pp. 161:1–161:10 (2025). <https://doi.org/10.1145/3757377.3763987>
2. Deng, J., Guo, J., Xue, N., Zafeiriou, S.: Arcface: Additive angular margin loss for deep face recognition. In: IEEE Conference on Computer Vision and Pattern Recognition, CVPR 2019, Long Beach, CA, USA, June 16-20, 2019. pp. 4690–4699. Computer Vision Foundation / IEEE (2019). <https://doi.org/10.1109/CVPR.2019.00482>
3. Frenkel, Y., Vinker, Y., Shamir, A., Cohen-Or, D.: Implicit style-content separation using b-lora. In: Leonardis, A., Ricci, E., Roth, S., Russakovsky, O., Sattler, T., Varol, G. (eds.) Computer Vision - ECCV 2024 - 18th European Conference, Milan, Italy, September 29-October 4, 2024, Proceedings, Part X. Lecture Notes in Computer Science, vol. 15068, pp. 181–198. Springer (2024). https://doi.org/10.1007/978-3-031-72684-2_11
4. Gal, R., Alaluf, Y., Atzmon, Y., Patashnik, O., Bermano, A.H., Chechik, G., Cohen-Or, D.: An image is worth one word: Personalizing text-to-image generation using textual inversion. In: International Conference on Learning Representations (ICLR) (2023)
5. Gu, Y., Wang, X., Wu, J.Z., Shi, Y., Chen, Y., Fan, Z., Xiao, W., Zhao, R., Chang, S., Wu, W., Ge, Y., Shan, Y., Shou, M.Z.: Mix-of-show: Decentralized low-rank adaptation for multi-concept customization of diffusion models. In: Oh, A., Naumann, T., Globerson, A., Saenko, K., Hardt, M., Levine, S. (eds.) Advances in Neural Information Processing Systems 36: Annual Conference on Neural Information Processing Systems 2023, NeurIPS 2023, New Orleans, LA, USA, December 10 - 16, 2023 (2023)
6. Hu, E.J., Shen, Y., Wallis, P., Allen-Zhu, Z., Li, Y., Wang, S., Wang, L., Chen, W.: Lora: Low-rank adaptation of large language models. In: The Tenth International Conference on Learning Representations, ICLR 2022, Virtual Event, April 25-29, 2022. OpenReview.net (2022)
7. Kong, Z., Zhang, Y., Yang, T., Wang, T., Zhang, K., Wu, B., Chen, G., Liu, W., Luo, W.: Omg: Occlusion-friendly personalized multi-concept generation in diffusion models. In: Computer Vision - ECCV 2024 - 18th European Conference, Milan, Italy, September 29-October 4, 2024, Proceedings, Part XXXI. Lecture Notes in Computer Science, vol. 15089, pp. 253–270. Springer (2024)
8. Kumari, N., Zhang, B., Zhang, R., Shechtman, E., Zhu, J.: Multi-concept customization of text-to-image diffusion. In: IEEE/CVF Conference on Computer Vision and Pattern Recognition, CVPR 2023, Vancouver, BC, Canada, June 17-24, 2023. pp. 1931–1941. IEEE (2023). <https://doi.org/10.1109/CVPR52729.2023.00192>
9. Li, Y., Liu, H., Wu, Q., Mu, F., Yang, J., Gao, J., Li, C., Lee, Y.J.: GLIGEN: open-set grounded text-to-image generation. In: IEEE/CVF Conference on Computer Vision and Pattern Recognition, CVPR 2023, Vancouver, BC, Canada, June 17-24, 2023. pp. 22511–22521. IEEE (2023). <https://doi.org/10.1109/CVPR52729.2023.02156>
10. Lungu-Stan, V.C., Mironică, I., Georgescu, M.I.: Lade: Unified multi-layered graphic media generation and decomposition. arXiv preprint arXiv:2603.17965 (2026)

11. Ouyang, Z., Li, Z., Hou, Q.: K-lora: Unlocking training-free fusion of any subject and style loras. In: IEEE/CVF Conference on Computer Vision and Pattern Recognition, CVPR 2025, Nashville, TN, USA, June 11-15, 2025. pp. 13041–13050. Computer Vision Foundation / IEEE (2025). <https://doi.org/10.1109/CVPR52734.2025.01217>
12. Po, R., Yang, G., Aberman, K., Wetzstein, G.: Orthogonal adaptation for modular customization of diffusion models. In: IEEE/CVF Conference on Computer Vision and Pattern Recognition, CVPR 2024, Seattle, WA, USA, June 16-22, 2024. pp. 7964–7973. IEEE (2024). <https://doi.org/10.1109/CVPR52733.2024.00761>
13. Radford, A., Kim, J.W., Hallacy, C., Ramesh, A., Goh, G., Agarwal, S., Sastry, G., Askell, A., Mishkin, P., Clark, J., Krueger, G., Sutskever, I.: Learning transferable visual models from natural language supervision. In: International Conference on Machine Learning (ICML) (2021)
14. Radford, A., Kim, J.W., Hallacy, C., Ramesh, A., Goh, G., Agarwal, S., Sastry, G., Askell, A., Mishkin, P., Clark, J., Krueger, G., Sutskever, I.: Learning transferable visual models from natural language supervision. In: Meila, M., Zhang, T. (eds.) Proceedings of the 38th International Conference on Machine Learning, ICML 2021, 18-24 July 2021, Virtual Event. Proceedings of Machine Learning Research, vol. 139, pp. 8748–8763. PMLR (2021)
15. Ruiz, N., Li, Y., Jampani, V., Pritch, Y., Rubinstein, M., Aberman, K.: Dreambooth: Fine tuning text-to-image diffusion models for subject-driven generation. In: IEEE/CVF Conference on Computer Vision and Pattern Recognition, CVPR 2023, Vancouver, BC, Canada, June 17-24, 2023. pp. 22500–22510. IEEE (2023). <https://doi.org/10.1109/CVPR52729.2023.02155>
16. Shah, V., Ruiz, N., Cole, F., Lu, E., Lazebnik, S., Li, Y., Jampani, V.: Ziplora: Any subject in any style by effectively merging loras. In: Leonardis, A., Ricci, E., Roth, S., Russakovsky, O., Sattler, T., Varol, G. (eds.) Computer Vision - ECCV 2024 - 18th European Conference, Milan, Italy, September 29-October 4, 2024, Proceedings, Part I. Lecture Notes in Computer Science, vol. 15059, pp. 422–438. Springer (2024). https://doi.org/10.1007/978-3-031-73232-4_24
17. Voynov, A., Chu, Q., Cohen-Or, D., Aberman, K.: P+: extended textual conditioning in text-to-image generation. CoRR **abs/2303.09522** (2023). <https://doi.org/10.48550/ARXIV.2303.09522>
18. Wu, C., Li, J., Zhou, J., Lin, J., Gao, K., Yan, K., Yin, S.m., Bai, S., Xu, X., et al.: Qwen-image technical report (2025)
19. Yin, S., Zhang, Z., Tang, Z., Gao, K., Xu, X., Yan, K., Li, J., Chen, Y., Chen, Y., Shum, H., Ni, L.M., Zhou, J., Lin, J., Wu, C.: Qwen-image-layered: Towards inherent editability via layer decomposition. arXiv preprint arXiv:2512.15603 (2025)
20. Zhang, L., Agrawala, M.: Transparent image layer diffusion using latent transparency. ACM Trans. Graph. **43**(4), 100:1–100:15 (2024). <https://doi.org/10.1145/3658150>

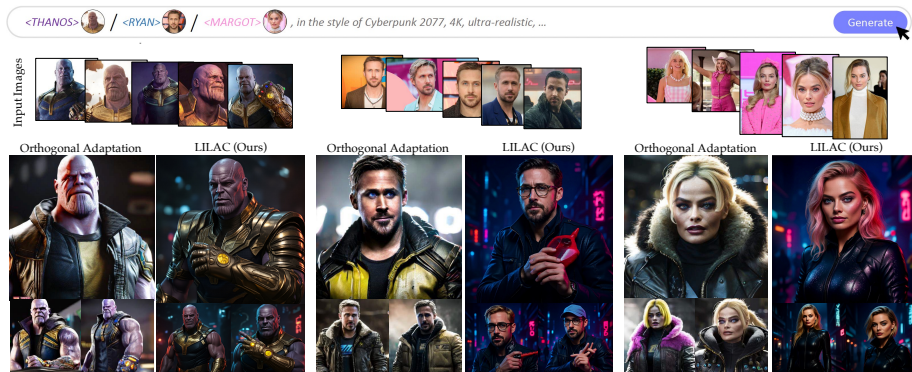


Fig. 6: Single-concept generations in the style of *Cyberpunk 2077* for three concepts: input references (top) and a comparison of Orthogonal Adaptation [12] with LILAC.

A Additional Qualitative Results

Beyond the multi-subject compositions of Fig. 4, we report single-concept renderings under a pronounced artistic style, a setting that stresses identity preservation because the style competes with each subject’s appearance. For three concepts, Fig. 6 shows the reference images together with generations from Orthogonal Adaptation [12] and from LILAC, so that per-concept fidelity can be compared directly.

B Implementation and Evaluation Details

Single-concept screening. Before composing concepts, we verify that each is faithfully captured in isolation: we generate every concept on its own and retain only those whose single-concept identity score clears a fixed threshold. A subject that an adapter cannot reconstruct alone cannot be expected to survive composition, so this screen removes single-concept training failures from the multi-subject evaluation and isolates the question we study, whether identities are preserved when several concepts are combined, from the separate question of whether each concept was learned well in the first place. Concepts that fail the screen are excluded from all multi-subject results.

Implementation details. On the open-source backbone, each concept adapter is a rank-64 LoRA on the MMDiT attention layers of Qwen-Image-Edit, trained for 1,000 steps with learning rate 10^{-4} and DreamBooth-style trigger-token binding on a blank source image, with the backbone frozen throughout. At composition time the anchor is the concept with the largest adapter delta norm $\|\Delta W\|_F$ (Sec. 3.3); each subsequent pass conditions on the frozen composite with a single adapter active, and no further optimization is performed. For evaluation we use CLIP ViT-B/32 (OpenAI) for the alignment metrics and InsightFace buffalo_1 (ArcFace) for identity, with the detection threshold of [12].

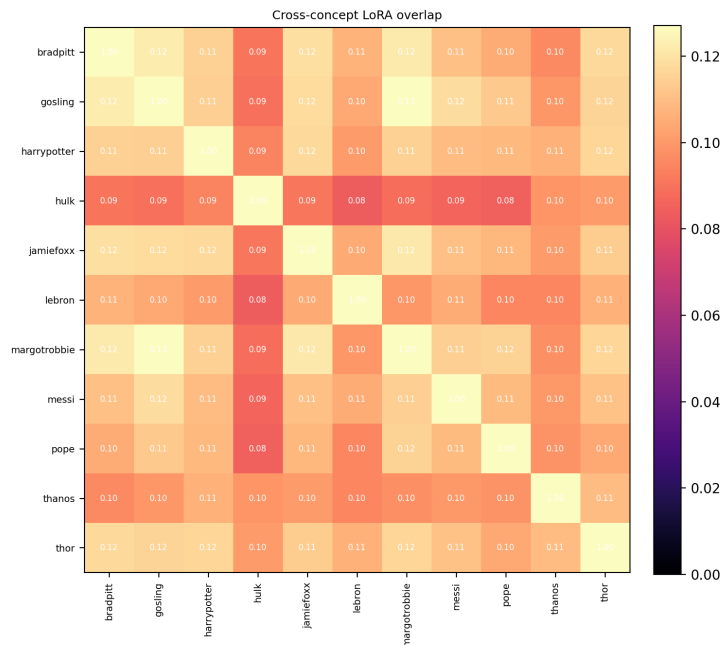


Fig. 7: Cross-concept overlap between the independently trained adapters. Each cell is the normalised overlap $ov_{ij} \in [0, 1]$ between the LoRA residuals of concepts i and j (1 on the diagonal; 0 for orthogonal residuals). Off-diagonal values average 0.106, $5.3\times$ the 0.020 chance level for random adapters of the same size: the residuals are not orthogonal. This is the crosstalk χ_{ij} that weight-space fusion must suppress and that per-layer binding never instantiates.

C Additional Quantitative Analyses

We visualize the cross-concept overlap between the independently trained adapters in Fig. 7; it underlies the binding argument of Sec. 3.5.

We report per-subject quality against the number of subjects in Fig. 8, supporting the scalability discussion of Sec. 4.4.

D Subject-Ordering Ablation

Sec. 3.3 orders the subjects of a composition by descending LoRA Frobenius norm, placing the strongest-adapter concept first. To test whether this heuristic matters, we fix a set of eight three-subject groups and compose each under three orderings: our default (anchor-first, descending $\|\Delta W\|_F$), its reverse (anchor-last, ascending), and a random permutation, holding every other setting identical. Tab. 2 reports the outcome. The three orderings fall within a narrow band on every metric (identity 0.82–0.85, image 0.72–0.77, text 0.69–0.71), so the method is largely robust to composition order. Within that band, anchor-first ties for the best identity and gives the best text alignment, a random order is marginally

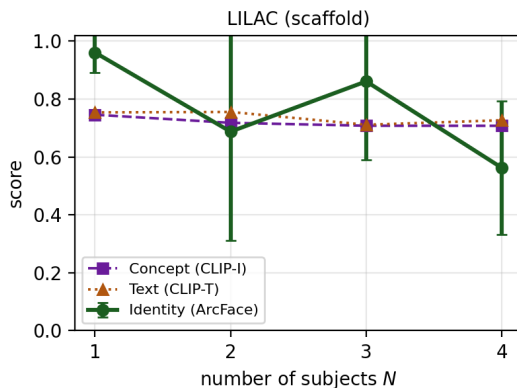


Fig. 8: Per-subject quality versus the number of subjects N (scaffold configuration); $N=1$ is the single-concept reference, averaged over the concept bank. Concept fidelity (CLIP-I) and text alignment (CLIP-T) stay flat as N grows, while the ArcFace detection rate is lower and noisier at larger N , reflecting scene crowding and smaller faces rather than identity blending. Error bars are ± 1 standard deviation, over random subject groups for $N \geq 2$ and over the concept bank at $N=1$.

Table 2: Effect of subject ordering on the scaffold configuration, over a fixed set of eight three-subject groups. Anchor-first (our default) orders subjects by descending LoRA Frobenius norm $\|\Delta W\|_F$. Best per column in bold; higher is better.

Ordering	Identity \uparrow	Image \uparrow	Text \uparrow
Random	0.850	0.766	0.687
Anchor-last (ascending)	0.822	0.730	0.709
Anchor-first (descending, ours)	0.850	0.723	0.714

ahead on concept fidelity, and anchor-last is weakest on identity. The margins are small (identity varies by under three points across orderings), so placing the strongest adapter first is a sound default rather than a critical choice, consistent with treating the order as a compositional-priority control (Sec. 3.3). Absolute scores here use a fixed eight-group subset and are not directly comparable to Tab. 1; only the relative ordering is meaningful.